


Assessment of Sympathetic Reinnervation After Cardiac Transplantation Using Hybrid Cardiac PET/MRI: A Pilot Study

Dietrich Beitzke, MD,^{1*}  Alice Wielandner, MD,¹ Tim Wollenweber, MD, DI,² Chrysoula Vraka, Dr,² Verena Pichler, Dr,² Keziban Uyanik-Uenal, MD,³ Andreas Zuckermann, MD,³ Andreas Greiser, DI,⁴ Marcus Hacker, MD,² and Christian Loewe, MD¹

Background: Sympathetic reinnervation after heart transplantation (HTX) is a known phenomenon, which has an impact on patient heart rate variability and exercise capacity. The impact of reinnervation on myocardial structure has not been evaluated yet.

Propose: To evaluate the feasibility of simultaneous imaging of cardiac reinnervation and cardiac structure using a hybrid PET/MRI system.

Study type: Prospective / pilot study.

Subjects: Ten patients, 4–21 years after cardiac transplantation.

Field Strength/Sequence: 3 T hybrid PET/MRI system. Cine SSFP, T₁ mapping (modified Look–Locker inversion recovery sequence) pre/postcontrast as well as dynamic [¹¹C]meta-hydroxyephedrine ([¹¹C]mHED) PET.

Assessment: All MRI and PET parameters were evaluated by experienced readers using dedicated postprocessing software packages for cardiac MRI and PET. For all parameters a 16-segment model for the left ventricle was applied.

Statistical Tests: Mann–Whitney *U*-test; Spearman correlations.

Results: Thirty-six of 160 myocardial segments showed evidence of reinnervation by PET. On a segment-based analysis, mean native T₁ relaxation times were nonsignificantly altered in segments with evidence of reinnervation (1305 ± 151 msec vs. 1270 ± 112 msec; *P* = 0.1), whereas mean extracellular volume (ECV) was significantly higher in segments with evidence of reinnervation (35.8 ± 11% vs. 30.9 ± 7%; *P* = 0.019). There were no significant differences in wall motion (WM) and wall thickening (WT) between segments with or without reinnervation (mean WM: 7.6 ± 4 mm vs. group B: 9.3 ± 7 mm [*P* = 0.13]; WT: 79 ± 63% vs. 94 ± 74% [*P* = 0.27]) under resting conditions.

Data Conclusion: The assessment of cardiac reinnervation using a hybrid PET/MRI system is feasible. Segments with evidence of reinnervation by PET showed nonsignificantly higher T₁ relaxation times and a significantly higher ECV, suggesting a higher percentage of diffuse fibrosis in these segments, without impairment of rest WM and WT.

Level of Evidence: 3

Technical Efficacy: Stage 3

J. MAGN. RESON. IMAGING 2019;50:1326–1335.

CARDIAC TRANSPLANT is a lifesaving procedure in patients with endstage heart disease. Due to the surgical procedure, which includes aortic cross-clamping, the graft becomes denervated from the autonomous nervous system by the time of the procedure. However, improved heart rate variability and imaging of the nerve metabolism by positron emission

View this article online at wileyonlinelibrary.com. DOI: 10.1002/jmri.26722

Received Dec 5, 2018, Accepted for publication Mar 2, 2019.

*Address reprint requests to: D.B., Department of Biomedical Imaging and Image-Guided Therapy, Division of Cardiovascular and Interventional Radiology, Medical University of Vienna, Waehringer Guertel 18-20, 1090 Vienna, Austria. E-mail: dietrich.beitzke@meduniwien.ac.at
The first two authors contributed equally to this work.

From the ¹Department of Biomedical Imaging and Image-Guided Therapy, Division of Cardiovascular and Interventional Radiology, Medical University of Vienna, Vienna, Austria; ²Department of Biomedical Imaging and Image-Guided Therapy, Division of Nuclear Medicine, Medical University of Vienna, Vienna, Austria; ³Department of Surgery, Division of Cardiac Surgery, Medical University of Vienna, Vienna, Austria; and ⁴Siemens Healthcare, Erlangen, Germany
This is an open access article under the terms of the Creative Commons Attribution-NonCommercial License, which permits use, distribution and reproduction in any medium, provided the original work is properly cited and is not used for commercial purposes.

tomography (PET) suggest that sympathetic reinnervation starts to reappear shortly after cardiac transplant.¹ Further, potential reinnervation of the allograft has been described to be beneficial for myocardial metabolism, blood flow, and exercise capacity.^{2,3} PET, using [¹¹C]meta-hydroxyephedrine ([¹¹C]mHED) to delineate the sympathetic nerve metabolism has been proven to depict allograft reinnervation over time and its effect on ventricular function under exercise conditions.²

Magnetic resonance imaging (MRI) is a well-established imaging technique and is increasingly used to follow up cardiac transplant patients to noninvasively evaluate cardiac function and myocardial tissue composition.^{4,5} In particular, the differentiation of ischemic or nonischemic patterns of late gadolinium enhancement (LGE) can help to differentiate scars from cardiac allograft vasculopathy (CAV) or fibrotic remnants from prior rejection episodes.⁶ With the introduction of T₁ mapping techniques using modified Look–Locker inversion recovery (MOLLI) sequences, the evaluation and quantification of diffuse cardiac diseases also became possible.⁷ In this setting an elevation of the native T₁ values represents changes in the myocardial composition, mainly fibrosis, amyloid deposition, or inflammation. On the other hand, a reduction of the T₁ value represents myocardial fat depositions (eg, Fabry's disease).⁸ Postcontrast T₁ maps enable the quantification of extracellular volume (ECV), mainly representing diffuse fibrosis solely, a biomarker for outcome in various cardiac diseases.⁹

Hybrid PET/MRI is a fairly new technology that combines standalone PET and MRI. Preliminary studies, mainly obtained with [¹⁸F]fluorodeoxyglucose ([¹⁸F]FDG) PET/MRI have shown mostly synergistic data in evaluating pathologies like acute myocardial ischemia.¹⁰ The aim of this pilot study, therefore, was to evaluate the feasibility of image cardiac reinnervation with hybrid PET/MRI and to obtain insights into the myocardial composition and function of reinnervated and denervated myocardial segments using modern cardiovascular magnetic resonance (CMR) techniques.

Materials and Methods

Fully-automated synthesis of [¹¹C]mHED was performed with a commercially available synthesizer, GE TRACERlab FX C Pro (Milwaukee, WI). [¹¹C]mHED was formulated exclusively with a 0.9% saline solution. The GMP-grade precursor metaraminol was purchased from ABX (Radeberg, Germany). Quality control was in accordance with the European Pharmacopoeia, including the parameters radiochemical, chemical purity, pH, osmolality, radionuclidic purity, residual solvents, as well as sterility and endotoxins.

Patients

Ten consecutive patients (nine male, one female) with a history of cardiac transplantation at least 3 years prior to the examination were included between May 2017 and April 2018. Exclusion criteria were claustrophobia, history of a pacemaker or ICD implantation into the

graft, abandoned pacemaker leads from old pacemaker systems, and severe renal insufficiency (defined as estimated glomerular filtration rate < 30 ml/min). The study was approved by the local Institutional Review Board / Ethics Committee of the Medical University of Vienna, Austria. All patients gave written, informed consent prior to study inclusion.

Patient characteristics (time to transplant, history of cardiac allograft vasculopathy, prior allograft rejection periods) were derived from patient records.

Patient Preparation and PET/MRI Examination

Patients were allowed to eat until 4 hours prior to the examination, but were asked to abstain from caffeine intake for 36 hours prior to PET/MRI. None of the patients received medication that would interfere with the presynaptic sympathetic nervous system (eg, antidepressants, clonidine), or beta or alpha blockade.

Imaging Protocol

All PET/MRI examinations were acquired on a simultaneous PET/MRI system (Biograph mMR; Siemens Healthcare, Erlangen, Germany). The technical details have been reported elsewhere.¹¹ Patients were positioned head-first, supine. An electrocardiogram (ECG) device was used for cardiac triggering. PET tracer and contrast agent were injected through a venous cannula.

MRI

MRI included balanced steady-state free precession (bSSFP) imaging in two-, three-, and four-chamber views, and left ventricular (LV) outflow tract and short axis for the evaluation of cardiac function. T₁-mapping, using a MOLLI prototype sequence pre- and postcontrast (Sampling Pattern 5(3)3/4(1)3(1)2; with motion correction) was used to determine the ECV on three short-axis slices located within the LV at the basal, mid-cavity, and apical positions.⁸ LGE imaging was performed in short-axis, two-, three-, and four-chamber views 10–15 minutes after the injection of 0.15 ml gadobutrol (0.1 mmol/ml) per kg bodyweight (Gadovist, Bayer, Berlin, Germany) using phase sensitive inversion recovery (PSIR) sequences.

PET

During MRI, mean 480 ± 103 MBq [¹¹C]HED was administered intravenously. A 40-minute PET acquisition was performed in listmode with ECG triggering. The imaging protocol is shown in Fig. 1.

Image Postprocessing

MRI. For MRI postprocessing, commercially available software was used (MR Suite, Medis; Leiden, Netherlands). LV and right ventricular (RV) volumes and function, as well as wall motion (WM) in mm and wall thickening (WT) in percent were derived from the end-diastolic and end-systolic phase using short-axis cine bSSFP images. Postschismic or diffuse scar was determined from the LGE images. A positive LGE was defined as a signal increase above the fifth standard deviation derived from remote myocardium.¹² Manual correction was performed to correct for artifacts. Scarring/fibrosis was calculated as the total amount of LV scarring in ml and percentage of LV mass. The ECV was calculated according to a standard formula from pre- and postcontrast

MRI	Planning: Scout scans	T2 HASTE	SSFP in SA, 2-, 3- and 4- chamber view	T1 mapping in 3 SA slices	Gd	LGE in SA, 2-, 3- and 4- chamber view w PSIR	T1 mapping in 3 SA slices
-----	--------------------------	-------------	---	------------------------------	----	---	------------------------------

PET	[¹¹ C]mHED (40 min dynamic acquisition)
-----	--

FIGURE 1: PET/MRI imaging protocol for assessment of myocardial fibrosis and reinnervation in cardiac transplant.

T₁ maps.⁸ All parameters were analyzed using a 16-segment myocardial model. Postprocessing of T₁ mapping is shown in Fig. 2. Images were read in concert by two experienced readers (A.W. and D.B.) with 5 and respectively 12 years of experience in cardiac MRI.

PET. Attenuation-corrected images were reconstructed in a 256 × 256 matrix. The dedicated Munich heart software was used for volumetric sampling and analysis of the spatial tracer retention in the ventricle.¹³ [¹¹C]mHED retention was quantified from dynamic images using a retention index (tissue activity from 30 to 40 min divided by the integral of the [¹¹C]mHED

activity input function; %/min).¹⁴ Myocardium with a [¹¹C]mHED retention index below 7%/min was defined as denervated, as described elsewhere.^{15,16} Thus, the extent of LV reinnervation was quantified by the percentage of the polar map with a retention index above 7%/min. For regional analysis, a 16-segment model similar to the MRI postprocessing was used and the mean retention index was calculated for each segment.

Statistical Analyses

All statistical analyses were performed using SPSS (SPSS Mac, v. 20.0; Chicago, IL). Continuous data were expressed as mean ± standard deviation (SD) and discrete data as frequencies and percentages. Further graphical correlations were obtained. Due to the small

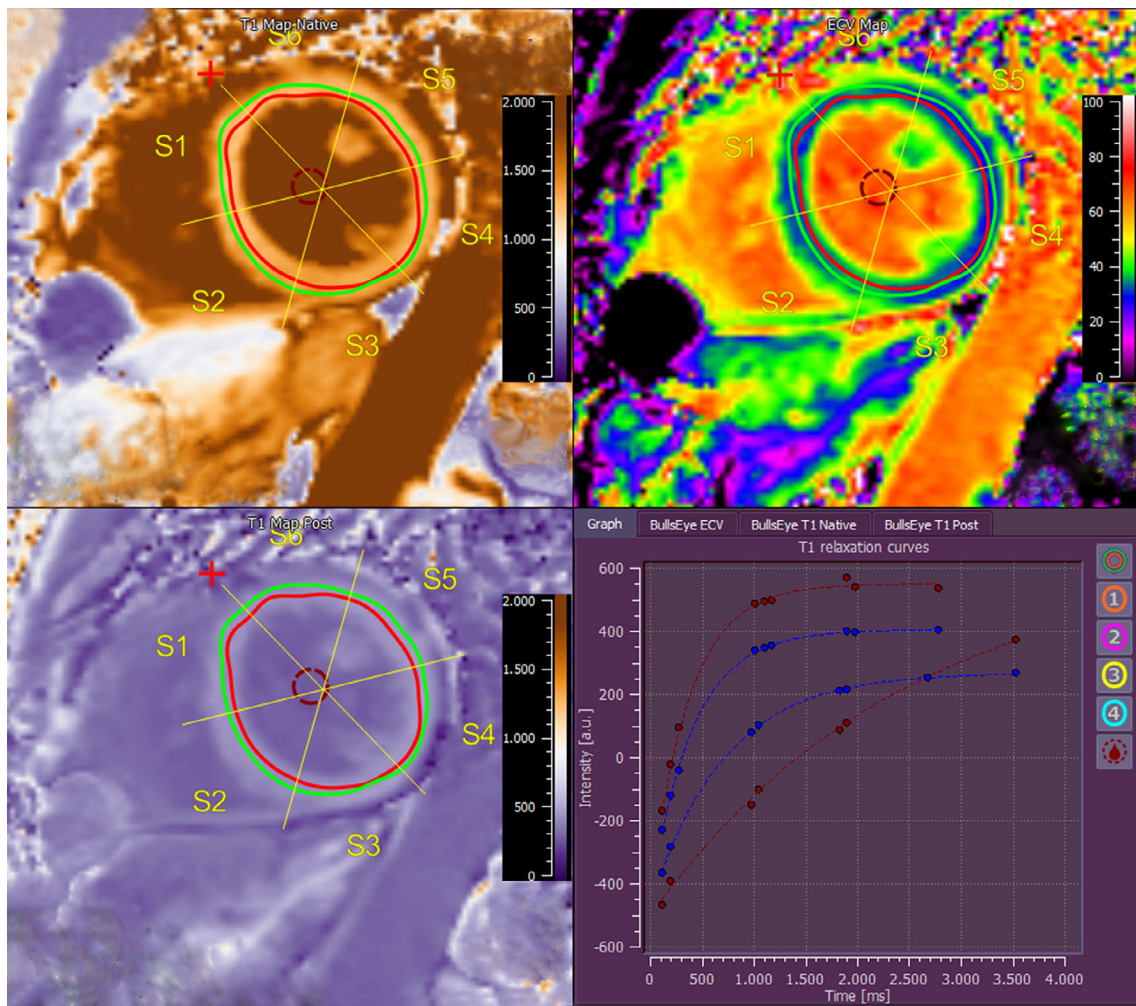


FIGURE 2: Image postprocessing of T₁ mapping: Endo- and epicardial borders are drawn within the myocardium to ensure a "virtual histology." Native and postcontrast T₁ maps are located on the left side. The composed T₁ map is shown on the upper right side. Representative slice from mid-cavity short axis.

sample size, a Mann–Whitney *U*-test was performed for group comparisons. For detailed analysis, myocardial segments were grouped according to the presence or absence of reinnervation on PET (defined by a cutoff index of 7% as described above). Further, segment-based Spearman correlations of [¹¹C]mHED uptake with years posttransplant, functional and morphologic parameters were obtained. *P* < 0.05 was considered statistically significant.

Results

Patient and Imaging Study Characteristics

Patient characteristics are listed in Table 1. Reasons for transplant were dilated cardiomyopathy (*n* = 6), ischemic cardiomyopathy (*n* = 2), arrhythmogenic right ventricular cardiomyopathy (*n* = 1), and congenital heart disease (*n* = 1). Two patients had a history of prior rejection, and one patient suffered from post-transplant lymphoma at the time of the study. Cardiac allograft vasculopathy was evident in one patient, resulting in a nonrecent myocardial infarction in the lateral wall. All patients were free of cardiac symptoms at the time of PET/MRI.

PET/MRI could be completed in nine patients; one patient interrupted the scan after the contrast application due to increasing back pain; therefore, the postcontrast T₁ mapping and LGE images were not available in this patient. In two other patients, the apical short-axis slices of postcontrast T₁ mapping were not usable due to blooming artifacts that arose from sternal cerclages.

LV Function and Structure by MRI

Mean heart rate during the MRI was 79 ± 18.5 bpm (68–130). Mean LV ejection fraction (EF) assessed by MRI was 65 ± 18% (13–81%). One patient showed an atrial flutter at the time of PET/MRI, resulting in a likely inaccurate low EF of 13% when assessed by MRI. Left ventricular volumes were within the normal range (Table 1). Mean LV end-diastolic mass was 139.7 ± 26.1 g (130–176 g); LV WM was 9 ± 6 mm (0–20 mm); mean WT was 90 ± 71% (–27 to 380%).

One patient showed an old, postischemic scar within the territory of the left circumflex artery due an occlusion based on known cardiac allograft vasculopathy. These segments (*n* = 3) were excluded from the T₁ and ECV analysis. All other patients were negative on LGE images. Overall, mean LV T₁ relaxation times were 1274 ± 116 msec (823–1934 msec), resulting in a mean LV ECV of 32 ± 8 (16–55). Throughout the whole cohort the mean ECV showed a moderate correlation with years after transplant (*k* = 0.647; *P* = 0.001).

Reinnervation by PET

Using the 16-segment model, an overall total of 160 segments were evaluated by PET. Applying a cutoff index of 7% [¹¹C]mHED retention, 36 segments were classified as reinnervated, whereas 124 segments showed no reinnervation. Two patients showed a complete absence of reinnervation over the whole LV. In the rest of the cohort, the mean number of reinnervated

segments was 4.5 (range, 1–9). Reinnervation was most commonly demonstrated as starting in the region of the anterior wall and spreading to the apex (Fig. 3). A descriptive group comparison between patients with and without reinnervation is given in Table 1. Both patients without evidence for reinnervation suffered from diabetes mellitus.

Segment-Based Reinnervation Analysis by PET/MRI

To evaluate the influence of reinnervation on myocardial function and structure, segments were divided in two groups according to the criteria described above for reinnervation. The functional parameters of WM and WT did not show any significant difference between the groups (WM: mean 8 ± 4 mm in segments with reinnervation vs. 9 ± 7 in segments without evidence of reinnervation [*P* = 0.13]; mean WT: 79 ± 63% in segments with reinnervation vs. 94 ± 74% in segments without evidence of reinnervation [*P* = 0.27]).

Differences in myocardial composition were observed. Native T₁ relaxation times (msec) were slightly higher within the reinnervated segments (mean 1305 ± 151 msec) when compared with the nonreinnervated segments (mean 1270 ± 112 msec; *P* = 0.1). The ECV derived from native T₁ and post-contrast T₁ mapping showed significantly higher ECV values within segments with evidence of reinnervation than in segments without reinnervation (36 ± 11% vs. 31 ± 7%; *P* = 0.019) (Table 2, Figs. 4–5).

Correlation of [¹¹C]mHED With Years Posttransplant, Functional and Morphologic Parameters

On a segment-based correlation of mean [¹¹C]mHED and years posttransplant, there was a slight increase of [¹¹C]mHED retention over time (*k* = 0.381, *P* = 0.311). Correlation of mean [¹¹C]mHED retention with morphologic (T₁, ECV) parameters showed a slight increase of mean T₁ with increased mean [¹¹C]mHED retention (*k* = 0.1, *P* = 0.053) and an increase of mean ECV with increased mean [¹¹C]mHED retention (*k* = 0.298, *P* = 0.001).

Discussion

The main findings of this study are: 1) Imaging of sympathetic cardiac reinnervation using a hybrid PET/MRI system is feasible and can be combined with a multiparametric MRI protocol for advanced tissue characterization by T₁ mapping and LGE. 2) Within this small study cohort, we could show that the imaging characteristics of reinnervated segments might differ from non-reinnervated segments, which suggests that reinnervation might have an influence on tissue composition. 3) Despite differences in myocardial composition, there was no impact of reinnervation on rest LV function, WM, or WT, even when assessed on the segmental level. Hybrid cardiac PET/MRI is a relatively novel imaging technique that provides the opportunity to obtain deep insights into myocardial composition; however, its clinical value

TABLE 1. Overview of Patient Characteristics and Group Comparison of Patients With or Without Reinnervation, Including Age, Gender, Medical History, and LV Parameters

Patient characteristics	All patients (<i>n</i> = 10)	Patients with evidence for reinnervation by PET (<i>n</i> = 8)	Patients without evidence for reinnervation by PET (<i>n</i> = 2)
Age at HTX (a)	47 ± 14 [19–64]	48 ± 10 (45–62)	41 ± 31 (19–64)
Time post HTX (a)	7.1 ± 4.9 [4–21]	7.6 ± 5.5 [4–21]	5 ± 1 [4–6]
Female/male	1:9	1:7	0:2
Indication for HTX (<i>n</i>)			
Dilated cardiomyopathy	6	6	0
Ischemic cardiomyopathy	2	1	1
Arrhythmogenic right ventricular cardiomyopathy	1	1	0
Congenital heart disease	1	0	1
Cold ischemic time (min)	213 ± 45 [139–296]	203 ± 39 (139–271)	259 ± 53 (221–296)
Patients with former rejection (<i>n</i>)	2	1	1
Evidence for CAV (<i>n</i>)	1	1	0
Hypertension	10	8	2
Hyperlipidemia	9	8	1
Diabetes mellitus	2	0	2
Immunosuppression: (<i>n</i>)			
Tacrolimus	7	6	1
Cyclosporine	2	2	
Everolimus	1	0	1
Corticosteroids	2	1	1
Mycophenolate mofetil	9	7	2
Mean number of segments reinnervated	5 ± 3 (2–11)	5 ± 3 (2–11)	0
Mean heart rate during MR	79 ± 19 (68–130)	81 ± 21 (68–130)	73 ± 3 (70–75)
LV ejection fraction (%)	65 ± 18 (13–81)	64 ± 21 (13–80)	69 ± 5 (65–72)
LV end-diastolic volume (ml)	111 ± 27 (76–170)	102 ± 18 (76–123)	143 ± 38 (116–170)
LV end-systolic volume (ml)	41 ± 27 (15–92)	39 ± 29 (15–107)	45 ± 19 (27–83)
LV stroke volume (ml)	70 ± 24 (16–94)	63 ± 20 (16–79)	97 ± 19 (27–83)
LV end-diastolic mass (g)	140 ± 26 (103–176)	137 ± 25 (103–176)	168 ± 11 (159–175)
Mean T1 (msec)	1280 ± 122 (823,8–1934)	1290 ± 125 (824–1934)	1192 ± 99 (949–1419)
Mean ECV (%)	32 ± 8 (16–55)	33 ± 9 (16–55)	32 ± 2 (23–37)

HTX = heart transplantation; LV = left ventricular; CAV = cardiac allograft vasculopathy, ECV = extracellular volume.

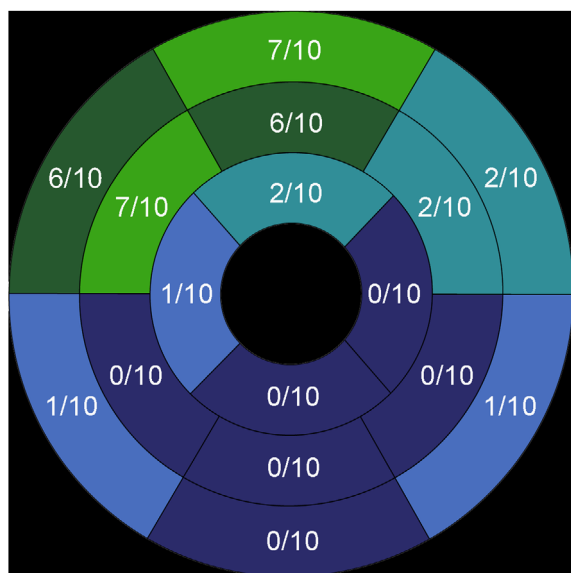


FIGURE 3: Distribution of LV cardiac reinnervation. Most of the segments with evidence of reinnervation were located on the anterior LV wall.

has yet to be evaluated.¹⁷ To date, most PET/MRI studies using [¹⁸F]FDG have focused on myocardial infarction or on the assessment of inflammation in the case of cardiac sarcoidosis.^{18,19} Nonetheless, LGE by MRI and missing or elevated [¹⁸F]FDG uptake often represent the same pathophysiological imaging targets, such as myocardial infarction or necrosis in the case of myocarditis. This might change when quantitative imaging by MRI and/or more specific tracers in PET are used.^{20,21}

Sympathetic cardiac reinnervation is a known phenomenon after cardiac transplant, which becomes assessable by orthostatic stress 5 months after transplant based on assessment of heart rate variability.²² Further, studies have shown that possible reinnervation seems to increase over time (as shown by [¹²³I]meta-iodobenzylguanidine ([¹²³I]MIBG) uptake in scintigraphy). For the process of reinnervation, sympathetic nerve fibers need to be connected to nerve terminals inside the transplanted heart.²³ However, sympathetic reinnervation does not occur in every patient and is not only time-dependent.²⁴ Two patients in our cohort showed no evidence of reinnervation (4 and 6 years after cardiac transplant). Factors that promote reinnervation include young donor age, young recipient age, and nonischemic cardiomyopathy as a reason for transplant. However, any form of allograft fibrosis or scar, as well as diabetes, have been described as unfavorable conditions for sympathetic reinnervation.^{24,25} Both of the patients without evidence of reinnervation had a history of type II diabetes that may have hindered reinnervation.

It has been shown by various studies that the presence of sympathetic reinnervation is of benefit for the patient in terms of resting heart rate and heart rate response to exercise.²⁶ When assessed by PET, reinnervation is often depicted in the anterior wall, including the anterior parts of the septum and anterolateral parts of the lateral wall. In our study, cohort reinnervation was most commonly found in the anterior wall.¹⁵

Imaging LV reinnervation by [¹¹C]mHED PET is a well-established and standardized imaging procedure. Using a cutoff of 7%/min [¹¹C]mHED retention within a myocardial segment is an accepted threshold to screen for reinnervation after cardiac transplant, and has been commonly used in various PET studies.^{2,15} It has also been shown by PET studies that reinnervation is beneficial for local blood flow via the release of norepinephrine from the reconnected sympathetic nerve terminals.³

After cardiac transplant, the allograft is exposed to multiple factors that promote the development of myocardial remodeling and fibrosis.²⁷ Whereas, in the early phase, reperfusion damage and rejection episodes alter the myocardial structure, cardiac allograft vasculopathy that results in ischemia further contributes to tissue remodeling of the allograft in the late phase.²⁸ Histological studies have shown that the degree of interstitial fibrosis in cardiac transplant patients increases during the years after transplant.²⁹ Gramley et al showed that, within a 10-year follow-up, the mean percentage of LV fibrosis increases from 12 up to 29%.²⁸ The authors proposed that, in addition to former rejection episodes, hypoxia and small vessel disease, mainly based on allograft vasculopathy, may play an essential role in this process. A correlation between years after transplant and an increase in ECV was also evident in our study cohort.

Assessment and quantification of diffuse myocardial fibrosis has become a main focus of MRI within the last decade. Using MOLLI sequences, it has become possible to quantify the extracellular volume and to differentiate between intra- and extracellular pathologies. The technology is currently undergoing histological verification in various cardiac diseases, such as amyloidosis and myocarditis.³⁰ T₁ mapping techniques have also been applied in the pediatric and adult transplant population.^{5,31} The degree of the ECV obtained by MRI has also already been correlated with the collagen volume fraction in endomyocardial biopsy. In a study of pediatric transplant recipients, Ide et al showed a moderate correlation between septal T₁ relaxation times and septal ECV by MRI and fibrosis markers in endomyocardial biopsy.⁵ The mean ECV values obtained by that study (30%) were quite similar to our study cohort; however, the authors did not use a 16-segment model.⁵ When compared with a normal cohort, Coelho-Filho et al also showed that ECV as a marker of tissue remodeling was increased in normal transplant recipients and even higher in those with rejection periods in the posttransplant history.⁴ An increase in ECV was also evident in this small cohort of long-term transplant survivors.

In our study, using mapping techniques and a 16-segment myocardial model, segments with evidence of reinnervation by PET, mainly located on the anterior wall, showed nonsignificantly higher T₁ relaxation times and significantly higher ECV when compared with segments without evidence of reinnervation. The fact that only ECV values were significantly different is probably based on that fact that the native T₁ signal including, besides the myocardium itself, blood flow, water, and

TABLE 2. Group Comparison of Reinnervated and Nonreinnervated Segments in Terms of T1 Relaxation Times, ECV, and Rest Function by WM and WT

	LV segments with evidence for reinnervation by PET	LV segments without evidence for reinnervation by PET	<i>P</i> -value
Number of segments (total 160)	36	124	NA
[¹¹ C]mHED (%)	9.6 ± 2	4 ± 1	NA
Excluded segments with positive LGE	0	3	NA
T1 relaxation time (msec)	1305 ± 151	1270 ± 113	0.13
ECV (%)	35 ± 11	31 ± 7	0.019*
WM (mm), mean ± SD	8 ± 4	9 ± 7	0.139
WT (%), mean ± SD	79 ± 63	94 ± 74	0.275

LGE = late gadolinium enhancement; ECV = extracellular volume; WM = Wall motion; WT = wall thickening.

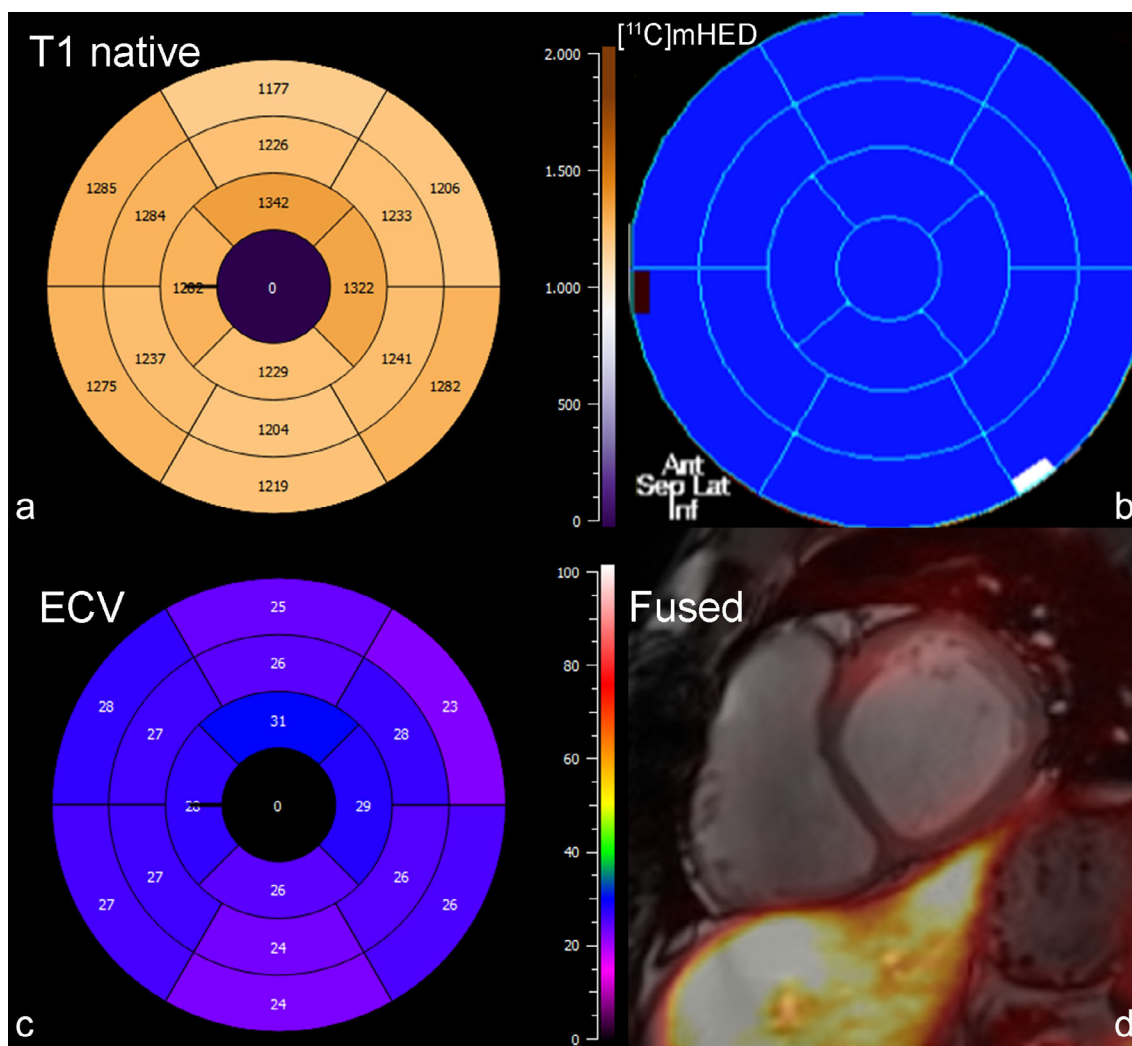


FIGURE 4: Bull's-eye plot of (a) native T₁ times, (b) reinnervated segments by [¹¹C]mHED, and (c) ECV in a 26-year-old male patient, 6 years after cardiac transplant. There is no evidence of reinnervation (b), and T₁ relaxation times, as well as the ECV distribution are homogeneous. Fused PET/MR image with no uptake in PET (d).

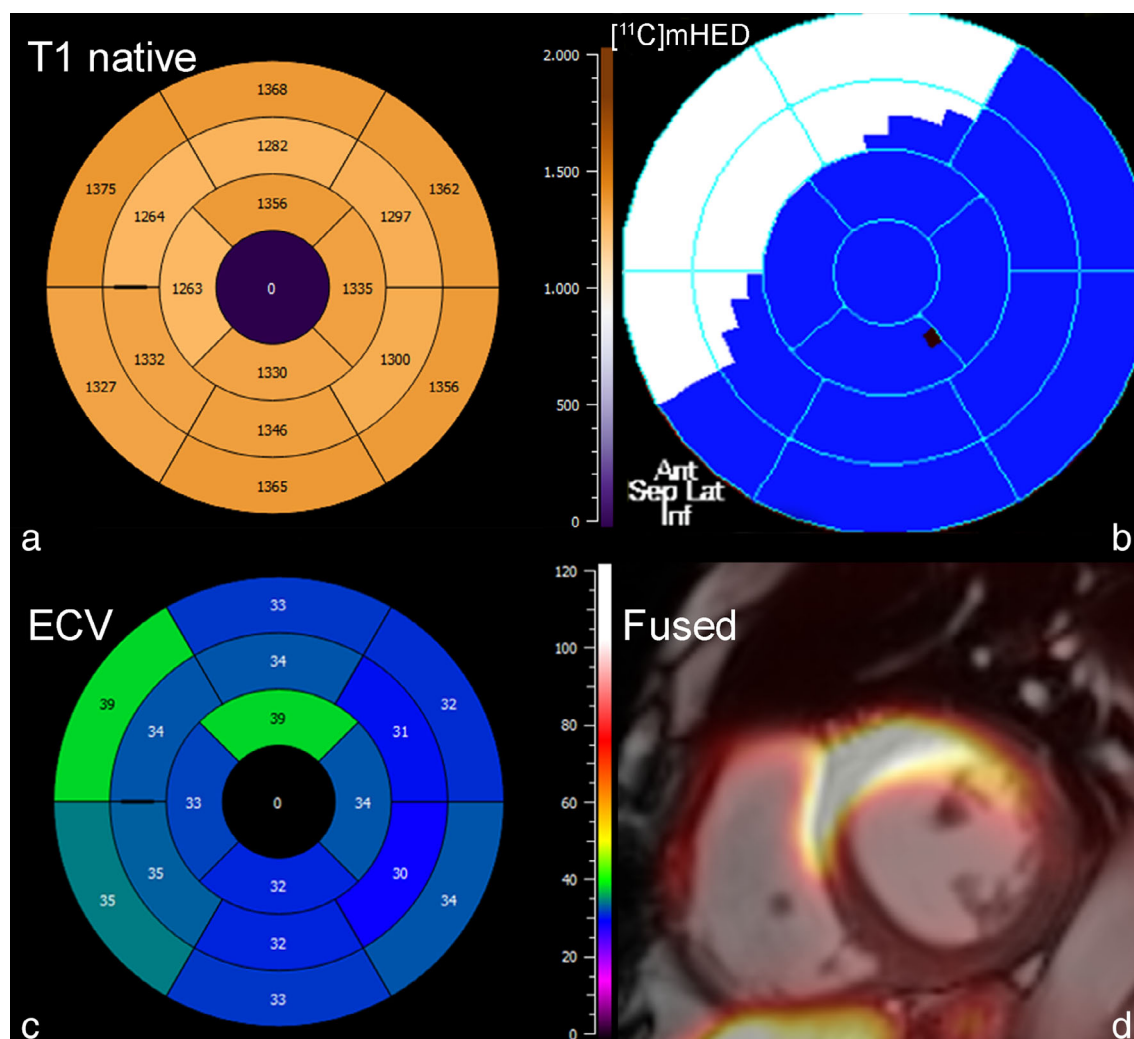


FIGURE 5: Bull's-eye plot of (a) native T₁ times, (b) reinnervated segments by [¹¹C]mHED, and (c) ECV in a 57-year-old female cardiac transplant patient, 6 years after heart transplantation. Segments with evidence of reinnervation over the anterior wall showed higher ECV values. Fused PET/MR image in (d).

fibrosis, whereas ECV is representing the extracellular space more exclusively, and therefore is more sensitive for fibrosis.³² In a study by Ellims et al, ECV and not native T₁ was well correlated with ventricular stiffness in a transplant cohort.³³

In addition, we could show, within this small cohort, that there is a weak correlation between overall [¹¹C]mHED retention (regardless of the 7% cutoff defining a segment as reinnervated) and native T₁ times, as well as the percentage of ECV by MRI. This suggests a link between the processes of reinnervation and tissue composition. The underlying potential mechanism for these findings remains unclear, but may be based on vascular pathologies implicating ischemia and fibrosis. Most of the literature on PET proposes an increased myocardial blood flow in patients with reinnervation, which suggests a protective mechanism of increased myocardial blood, thereby avoiding ischemia and the induction of fibrosis.³ Nonetheless, this has not been assessed on a segmental level as in our study, until now. Kushwaha et al evaluated myocardial perfusion in cardiac transplant patients at different timepoints after transplant.³⁴ The

authors showed that myocardial blood flow and its response to vasodilatation changed over the time, resulting in a decreased myocardial blood flow at rest and a decreased response to adenosine in patients more than 3 years after cardiac transplant.³⁴ An immune-mediated mechanism that could have caused endothelial dysfunction was proposed by the authors, but fibrosis, such as that in our cohort, may also play a role. Parallel monitoring of cardiac reinnervation was missing in that study; therefore, the potential link between cardiac reinnervation and a change in blood flow remains unclear. In a recent publication, Vermes et al applied a 16-segment model to patients after cardiac transplant when looking at acute rejection.³⁵ The study reported the basal segments to be more affected by edema and ECV elevation in patients with acute rejection. Therefore, fibrotic changes from prior rejection periods might also have affected basal ECV values in our study, as both patients with known rejection periods showed signs of reinnervation in PET. However, we observed a more accentuated increase in ECV over the basal anterior segments. Other technical issues may arise from MRI. Measuring

the ECV on MRI in the short axis located at the base and apex of the LV is not the standard procedure recommended in the guidelines, but this has already been validated in healthy subjects.^{8,36} Higher native T₁ relaxation times over the anterior wall in our cohort might also have been caused by an increased blood flow based on reinnervation, as shown by Reiter et al, who compared intraindividual end-systolic and end-diastolic T₁ relaxation times.³⁷ However, this would not explain an increased ECV after contrast application. Accordingly, the mechanism of the increased ECV in our population remains unclear and the link between reinnervation and potential induction myocardial fibrosis is still missing.

Our study has several limitations. First, the study is a proof-of-concept, pilot study that included a very small cohort of only 10 patients. Statistical significance was not reached on multiple parameters, and therefore the analyses might also be influenced by type II error. Patients included in the study had a long range of posttransplant years from 4–21 years and included patients with evidence of CAV and former rejection periods. Therefore, multiple factors influenced the tissue composition and reinnervation (eg, donor age, aortic clamp time, cold ischemic time).³⁸ In addition, the intrasubject variability, a topic of recent publications in transplant patients, was also not taken into account in our work due to the small sample size.^{35,36}

Furthermore, WM and WT were evaluated only under resting conditions and assessment of myocardial inflammation by T₂ mapping was not performed in our study.

In conclusion, our preliminary data show that imaging cardiac reinnervation after cardiac transplant using a hybrid PET/MRI system is feasible. On a segmental level, cardiac reinnervation might have an influence on tissue composition, with higher ECV values within segments that showed evidence of reinnervation on PET. There was also a correlation between [¹¹C]mHED uptake and elevated ECV throughout all segments. Further studies with appropriate sample sizes and more homogeneous patient cohorts need to be conducted to verify these preliminary data. In addition to evaluating cardiac transplants, hybrid cardiac PET/MRI using [¹¹C]mHED and T₁ mapping techniques might also be a useful tool in other cardiac diseases, such as dilative cardiomyopathy or inflammatory diseases in order to link denervation and diffuse fibrosis.

Acknowledgment

The authors thank the radiographer team at the local PET/MRI unit for their continuous effort and patience.

References

- Bernardi L, Bianchini B, Spadacini G, et al. Demonstrable cardiac reinnervation after human heart transplantation by carotid baroreflex modulation of RR interval. *Circulation* 1995;92:2895–2903.
- Bengel FM, Ueberfuhr P, Schiepel N, Nekolla SG, Reichart B, Schwaiger M. Effect of sympathetic reinnervation on cardiac performance after heart transplantation. *N Engl J Med* 2001;345:731–738.
- Di Carli MF, Tobes MC, Mangner T, et al. Effects of cardiac sympathetic innervation on coronary blood flow. *N Engl J Med* 1997;336:1208–1216.
- Coelho-Filho OR, Shah R, Lavagnoli CFR, et al. Myocardial tissue remodeling after orthotopic heart transplantation: A pilot cardiac magnetic resonance study. *Int J Cardiovasc Imaging* 2018;34:15–24.
- Ide S, Riesenkampff E, Chiasson DA, et al. Histological validation of cardiovascular magnetic resonance T1 mapping markers of myocardial fibrosis in paediatric heart transplant recipients. *J Cardiovasc Magn Reson* 2017;19:10.
- Braggion-Santos MF, Lossnitzer D, Buss S, et al. Late gadolinium enhancement assessed by cardiac magnetic resonance imaging in heart transplant recipients with different stages of cardiac allograft vasculopathy. *Eur Heart J Cardiovasc Imaging* 2014;15:1125–1132.
- Schelbert EB, Messroghli DR. State of the art: Clinical applications of cardiac T1 mapping. *Radiology* 2016;278:658–676.
- Messroghli DR, Moon JC, Ferreira VM, et al. Clinical recommendations for cardiovascular magnetic resonance mapping of T1, T2, T2* and extracellular volume: A consensus statement by the Society for Cardiovascular Magnetic Resonance (SCMR) endorsed by the European Association for Cardiovascular Imaging. *J Cardiovasc Magn Reson* 2017;19:75.
- Wong TC, Piehler K, Meier CG, et al. Association between extracellular matrix expansion quantified by cardiovascular magnetic resonance and short-term mortality. *Circulation* 2012;126:1206–1216.
- Nensa F, Poeppel TD, Beiderwellen K, et al. Hybrid PET/MR imaging of the heart: Feasibility and initial results. *Radiology* 2013;268:366–373.
- Torigian DA, Zaidi H, Kwee TC, et al. PET / MR imaging: Technical aspects and potential clinical applications. *Radiology* 2013;267:26–44.
- Bondarenko O, Beek AM, Hofman MBM, et al. Standardizing the definition of hyperenhancement in the quantitative assessment of infarct size and myocardial viability using delayed contrast-enhanced CMR. *J Cardiovasc Magn Reson* 2005;7:481–485.
- Nekolla SG, Miethaner C, Nguyen N, Ziegler SI, Schwaiger M. Reproducibility of polar map generation and assessment of defect severity and extent assessment in myocardial perfusion imaging using positron emission tomography. *Eur J Nucl Med* 1998;25:1313–1321.
- Allman KC, Stevens MJ, Wieland DM, et al. Noninvasive assessment of cardiac diabetic neuropathy by carbon-11 hydroxyephedrine and positron emission tomography. *J Am Coll Cardiol* 1993;22:1425–1432.
- Bengel FM, Ueberfuhr P, Ziegler SI, Nekolla S, Reichart B, Schwaiger M. Serial assessment of sympathetic reinnervation after orthotopic heart transplantation. A longitudinal study using PET and C-11 hydroxyephedrine. *Circulation* 1999;99:1866–1871.
- Schwaiger M, Hutchins GD, Kalf V, et al. Evidence for regional catecholamine uptake and storage sites in the transplanted human heart by positron emission tomography. *J Clin Invest* 1991;87:1681–1690.
- Nensa F, Bamberg F, Rischpler C, et al. Hybrid cardiac imaging using PET/MRI: A joint position statement by the European Society of Cardiovascular Radiology (ESCR) and the European Association of Nuclear Medicine (EANM). *Eur Radiol* 2018;28:4086–4101.
- Rischpler C, Dirschinger RJ, Nekolla SG, et al. Prospective evaluation of 18F-fluorodeoxyglucose uptake in postischemic myocardium by simultaneous positron emission tomography/magnetic resonance imaging as a prognostic marker of functional outcome. *Circ Cardiovasc Imaging* 2016;9:e004316.
- Schneider S, Batrice A, Rischpler C, Eiber M, Ibrahim T, Nekolla SG. Utility of multimodal cardiac imaging with PET/MRI in cardiac sarcoidosis: Implications for diagnosis, monitoring and treatment. *Eur Heart J* 2014;35:312.
- Kunze KP, Dirschinger RJ, Kossmann H, et al. Quantitative cardiovascular magnetic resonance: Extracellular volume, native T1 and 18F-FDG PET/CMR imaging in patients after revascularized myocardial infarction and association with markers of myocardial damage and systemic inflammation. *J Cardiovasc Magn Reson* 2018;20:33.

21. Rischpler C, Nekolla SG, Kossmann H, et al. Upregulated myocardial CXCR4-expression after myocardial infarction assessed by simultaneous GA-68 pentixafor PET/MRI. *J Nucl Cardiol* 2016;23:131–133.
22. Doering LV, Dracup K, Moser DK, Czer LSC, Peter CT. Hemodynamic adaptation to orthostatic stress after orthotopic heart transplantation. *Hear Lung J Acute Crit Care* 1996;25:339–351.
23. de Marco T, Dae M, Yuen-Green MSF, et al. Iodine-123 metaiodobenzylguanidine scintigraphic assessment of the transplanted human heart: Evidence for late reinnervation. *J Am Coll Cardiol* 1995; 25:927–931.
24. Bengel FM, Ueberfuhr P, Hesse T, et al. Clinical determinants of ventricular sympathetic reinnervation after orthotopic heart transplantation. *Circulation* 2002;106:831–835.
25. Bengel FM, Ueberfuhr P, Schäfer D, Nekolla SG, Reichart B, Schwaiger M. Effect of diabetes mellitus on sympathetic neuronal regeneration studied in the model of transplant reinnervation. *J Nucl Med* 2006;47:1413–1419.
26. Awad M, Czer LSC, Hou M, et al. Early denervation and later reinnervation of the heart following cardiac transplantation: A review. *J Am Heart Assoc* 2016;e004070.
27. Pichler M, Rainer PP, Schauer S, Hoefler G. Cardiac fibrosis in human transplanted hearts is mainly driven by cells of intracardiac origin. *J Am Coll Cardiol* 2012;59:1008–1016.
28. Gramley F, Lorenzen J, Pezzella F, et al. Hypoxia and myocardial remodeling in human cardiac allografts: A time-course study. *J Heart Lung Transplant* 2009;28:1119–1126.
29. Armstrong AT, Binkley PF, Baker PB, Myerowitz PD, Leier CV. Quantitative investigation of cardiomyocyte hypertrophy and myocardial fibrosis over 6 years after cardiac transplantation. *J Am Coll Cardiol* 1998;32:704–710.
30. Lurz P, Luecke C, Eitel I, et al. Comprehensive cardiac magnetic resonance imaging in patients with suspected myocarditis: The MyoRacer-Trial. *J Am Coll Cardiol* 2016;67:1800–1811.
31. Butler CR, Savu A, Bakal JA, et al. Correlation of cardiovascular magnetic resonance imaging findings and endomyocardial biopsy results in patients undergoing screening for heart transplant rejection. *J Heart Lung Transplant* 2015;34:643–650.
32. Lurz JA, Luecke C, Lang D, et al. CMR-derived extracellular volume fraction as a marker for myocardial fibrosis: The importance of coexisting myocardial inflammation. *JACC Cardiovasc Imaging* 2018;11:38–45.
33. Ellims AH, Shaw JA, Stub D, et al. Diffuse myocardial fibrosis evaluated by post-contrast T1 mapping correlates with left ventricular stiffness. *J Am Coll Cardiol* 2014;63:1112–1118.
34. Kushwaha SS, Narula J, Narula N, et al. Pattern of changes over time in myocardial blood flow and microvascular dilator capacity in patients with normally functioning cardiac allografts. *Am J Cardiol* 1998;82:1377–1381.
35. Vermes E, Pantaléon C, Auvet A, et al. Cardiovascular magnetic resonance in heart transplant patients: Diagnostic value of quantitative tissue markers: T2 mapping and extracellular volume fraction, for acute rejection diagnosis. *J Cardiovasc Magn Reson* 2018;20:59.
36. Weingärtner S, Meßner NM, Budjan J, et al. Myocardial T1-mapping at 3T using saturation-recovery: Reference values, precision and comparison with MOLLI. *J Cardiovasc Magn Reson* 2016;18:1–9.
37. Reiter U, Reiter G, Dorr K, Greiser A, Maderthaner R, Fuchsjaeger M. Normal diastolic and systolic myocardial T1 values at 1.5-T MR imaging: Correlations and blood normalization. *Radiology* 2014;271:365–372.
38. Estorch M, Campreciós M, Flotats A, et al. Sympathetic reinnervation of cardiac allografts evaluated by 123I-MIBG imaging. *J Nucl Med* 1999;40:911–916.